

# An Interaction Screen Identifies *headcase* as a Regulator of Large-Scale Pruning

Nicolas Loncle and Darren W. Williams

Medical Research Council Centre for Developmental Neurobiology, King's College London, London SE1 1UL, United Kingdom

Large-scale pruning, the removal of long neuronal processes, is deployed widely within the developing nervous system and is essential for proper circuit formation. In *Drosophila* the dendrites of the class IV dendritic arborization sensory neuron *ddaC* undergo large-scale pruning by local degeneration controlled by the steroid hormone ecdysone. The molecular mechanisms that control such events are largely unknown.

To identify new molecules that orchestrate this developmental degeneration, we performed a genetic interaction screen. Our approach combines the strength of *Drosophila* forward genetics with detailed *in vivo* imaging of *ddaC* neurons. This screen allowed us to identify *headcase* (*hdc*) as a new gene involved in dendrite pruning. *hdc* is evolutionarily conserved, but the protein's function is unknown. Here we show that *hdc* is expressed just before metamorphosis in sensory neurons that undergo remodeling. *hdc* is required in a cell-autonomous manner to control dendrite severing, the first phase of pruning. Our epistasis experiments with known regulators of dendrite pruning reveal *hdc* as a founding member of a new pathway downstream of ecdysone signaling.

## Introduction

In recent years our understanding of neural development has increased dramatically (Mason, 2009), but we still know relatively little about the cellular and molecular mechanisms that control neuron pruning (Luo and O'Leary, 2005). Large-scale pruning, where long neuronal processes are removed, is deployed widely within the developing nervous system and is essential for the proper construction of neural circuits. The best studied example occurs during the development of cortical layer 5 projection neurons whose subcortical axons undergo a branch-specific pruning, dependent on their region of origin (Stanfield et al., 1982). Data from retinal ganglion cells (Nakamura and O'Leary, 1989) and thalamocortical neurons (Portera-Cailliau et al., 2005) reveal that pruned axons are removed by local degeneration, not by distal to proximal branch retraction.

In insects that undergo a complete metamorphosis, a number of larval neurons are remodeled during the pupal–adult transition to become incorporated into adult circuits (Truman and Reiss, 1976; Truman, 1990). Pioneering studies of *Drosophila* mushroom body  $\gamma$ -neurons ( $\gamma$ -MB) reveal that both axons and dendrites prune by local degeneration (Watts et al., 2003). Detailed observations of these events show that branch thinning is coincident with changes in the microtubule cytoskeleton, fol-

lowed by severing and fragmentation. These features are also evident in the remodeling of sensory neuron dendrites (Kuo et al., 2005; Williams and Truman, 2005).

During metamorphosis, pruning is gated by a nuclear hormone receptor complex containing the ecdysone receptor (EcR) and ultraspiracle (*usp*), the fly RXR homolog (Schubiger et al., 1998). This nuclear receptor complex detects changes in the titer of the steroid hormone 20-hydroxy ecdysone (referred to hereafter as ecdysone). The loss of either partner results in a complete block of the pruning (Schubiger et al., 1998; Lee et al., 2000). The transcription factor Sox14, a downstream target of EcR, has recently been identified as a regulator of branch severing in a pathway that includes the large multidomain cytosolic protein Mical (Kirilly et al., 2009). Alongside this, a small number of other molecules have been identified as players in the pruning pathway, including components of the ubiquitin proteasome system (UPS) (Watts et al., 2003; Kuo et al., 2006), caspases (Kuo et al., 2006; Williams et al., 2006), *ik2*, and *Kat60L* (Lee et al., 2009). Nevertheless, the relationship between these molecules remains unclear.

To identify new molecules that orchestrate large-scale pruning and find links between known players, we developed a genome-wide interaction screen. This combines the strength of *Drosophila* forward genetics with detailed *in vivo* imaging of class IV dendritic arborizing (*da*) sensory neurons. Using this approach, we identified a novel regulator of pruning encoded by the gene called *headcase* (*hdc*). By developing new tools to test the requirement of pruning regulators in class IV *da* neurons, we have shown that *hdc* acts in a cell-autonomous manner to control the severing of primary dendrites in sensory neurons. Epistatic experiments reveal that *hdc* belongs to a new pathway downstream of the ecdysone receptor, independent of the transcription factor Sox14.

Received March 20, 2012; revised Sept. 17, 2012; accepted Sept. 24, 2012.

Author contributions: N.L. and D.W. designed research; N.L. performed research; N.L. and D.W. analyzed data; N.L. and D.W. wrote the paper.

This work was funded by the Medical Research Council and the Wellcome Trust. We thank Shigeo Hayashi, Ginés Morata, Christos Samakovlis, Rob White, Fengwei Yu, the NIG-FLY (Fly Stocks of National Institute of Genetics, Japan), the Vienna *Drosophila* RNAi Center, and the Bloomington Stock Center for generously providing fly stocks and other reagents. We also thank David Brierley, Muriel Boube, Matthias Landgraf, and Margrit Schubiger for helpful comments and suggestions on the manuscript.

Correspondence should be addressed to Dr. Nicolas Loncle at the above address. E-mail: nicolas.loncle@kcl.ac.uk.  
DOI:10.1523/JNEUROSCI.1391-12.2012

Copyright © 2012 the authors 0270-6474/12/3217086-11\$15.00/0

## Materials and Methods

**Fly stocks.** In this study *Drosophila* of either sex were used.

The following GAL4 driver strains were used: C161-GAL4 (Shepherd and Smith, 1996), expressed in five dorsal da neurons; ppk1.9-GAL4 driver (Grueber et al., 2003), expressed in ddaC and occasionally in isolated epidermal cells; 201Y-GAL4 (Yang et al., 1995), expressed in  $\gamma$ -MB neurons; and *elav*<sup>C155</sup>-GAL4, a general neuronal driver (Lin et al., 1994).

For this study we used the following flies: *hdc*<sup>43</sup> and *hdc*<sup>50</sup> (Weaver and White, 1995); UAS-*hdc* $\Delta$ 2 and UAS-*hdc* (Steneberg et al., 1998); UAS-*EcR*-RNAi<sup>CA104</sup> (Schubiger et al., 2005); UAS-*Sox14*, *Mical*<sup>15256</sup> (Kirilly et al., 2009); UAS-*Sp1*-RNAi and UAS-*btd*-RNAi (Estella et al., 2003); *Esg*<sup>G66B</sup> FRT40A (Hayashi, 1996); UAS-*Brm*<sup>DN</sup> (K804R) (Elfring et al., 1998); and CBP- $\Delta$ Q (Kumar et al., 2004). UAS-*hdc*-RNAi-15532R2 was obtained from the National Institute of Genetics (Japan). UAS-*Sox14*-RNAi-10856GD and UAS-*Mical*-RNAi-105837KK were obtained from the Vienna *Drosophila* RNAi Centre. The RNAi lines used for the screen were obtained from the National Institute of Genetics (Japan) and the Vienna *Drosophila* RNAi Centre (Dietzl et al., 2007). Deficiencies used for the screen were obtained from Bloomington Stock Center (<http://flystocks.bio.indiana.edu>), as well as the following flies, UAS-*Dicer2*, *hs-FLP*<sup>122</sup>, and *Ecr*<sup>m554fs</sup>.

**Mosaic analysis with a repressible cell marker.** For mosaic analysis with a repressible cell marker (MARCM) (Lee and Luo, 1999) of da sensory neurons, clones were induced in the embryo by a double heat shock method (Grueber et al., 2002). The following flies were generated: female: w, *elav*<sup>C155</sup>-GAL4, UAS-*RedStinger*, *hs-FLP*<sup>122</sup>; /+; FRT82B, tub-GAL80/TM6B Tb cross with male: w; ppk-eGFP; FRT82B *hdc*<sup>43</sup>/TM6B Tb and female: w, *elav*<sup>C155</sup>-GAL4, UAS-*redstinger*, *hs-FLP*<sup>122</sup>; FRT40A tub-GAL80/CyO to cross with male: w/w; *esg*<sup>G66B</sup> FRT40A/CyO; ppk-eGFP.

ddaC neurons were identified at 18 h after puparium formation (APF) by the ppk-eGFP, with MARCM clones expressing a nuclear RedStinger reporter protein.

For the MARCM analysis of the gamma MB neurons, the clones were induced in first instar larvae by applying a 1 h heat shock at 37°C as described previously (Lee et al., 1999; Lee and Luo, 1999) with female:  $\gamma$ , w, *hs-FLP*; 201Y-GAL4, mCD8-GFP/CyO; FRT82B, tub-GAL80/TM6B Tb.

**Staging of animals.** Individual animals were collected at pupariation and maintained at 25°C in a Petri dish with moist filter paper. Staging was denoted as hours after puparium formation or APF.

**Immunocytochemistry.** Immunocytochemistry was performed as described by Truman et al. (2004). Primary antibodies used were rabbit anti-GFP diluted 1/500 (Invitrogen), mouse-anti HDC mAb U33.7 diluted 1:5 and kindly provided by Robert White (University of Cambridge, Cambridge, UK) (Weaver and White, 1995), and mouse anti-*Sox14* diluted 1:200 kindly provided by Fengwei Yu (National University of Singapore, Singapore) (Kirilly et al., 2009).

Secondary antibodies used were FITC donkey anti-rabbit IgG diluted 1:500 from Jackson ImmunoResearch Laboratories and Cy3-conjugated donkey anti-rat or anti-mouse IgG diluted 1:500 Stratech Scientific.

**Imaging, image analysis, and quantification.** Confocal images were taken at 1  $\mu$ m intervals using a Zeiss LSM 510 system.

Stacks were assembled in NIH ImageJ (<http://rsb.info.nih.gov/ij/>). Images were adjusted only for brightness and contrast using Adobe Photoshop (Adobe Systems).

Third-instar larvae, white pre-pupae, and pupae until 12 h APF were directly imaged using confocal microscopy. After 12 h APF, pupae were peeled out of the pupal case. Images of neurons were taken as maximum projections of 15–40 optical sections at 1  $\mu$ m intervals. Quantification of all live images was carried out by counting the number of primary and secondary dendrites in a 230  $\times$  230  $\mu$ m region of the dendritic field of the ddaC neurons, originating from the second to fifth abdominal segments.

**Statistical analyses.** Mann–Whitney and Kruskal–Wallis statistical tests were performed in Graphpad Prism 5 with values of  $p < 0.05$  deemed to be significant.

## Results

### A genetic interaction screen to uncover molecules that control large-scale pruning

A number of larval sensory neurons in *Drosophila* undergo remodeling during metamorphosis to become components of the adult nervous system (Williams and Shepherd, 1999). This remodeling is achieved by the removal of larval arborizations followed by the outgrowth of adult-specific processes (Williams and Truman, 2004). Dorsal dendritic arborizing sensory neuron C (ddaC) is a class IV dendritic arborizing neuron located in the dorsal body wall of each larval hemisegment. ddaC pruning takes place in two distinct phases: severing and clearance. The first phase begins at the onset of metamorphosis at 0 h after puparium formation, APF. At this time, the proximal dendrites of ddaC begin to thin and form bead-like structures (Fig. 1A). By 10 h APF (Fig. 1B), 80% of the primary dendrites are severed ( $n = 50$ ). In the second phase of pruning, these severed dendrites are removed. By 18 h APF, the dendrites of ddaC have been completely removed in 85% of the dorsal body wall territories examined ( $n = 50$ ) (Fig. 1C). The remaining 15% of dorsal fields contain only a few small pieces of the severed dendrites that are soon removed (Fig. 1C). The timing of these events relative to puparium formation is highly stereotyped.

Relatively few molecules involved in large-scale pruning have been identified (Fig. 1D). To isolate novel regulators, we designed a genetic interaction screen. As the ecdysone receptor is at the apex of this pathway (Fig. 1E), we used it to generate a sensitized background. We recombined the null allele *Ecr*<sup>M554fs</sup> with ppk-GAL4 > CD8::GFP to visualize ddaC neurons directly in live animal. Flies heterozygous for *EcR* show normal pruning. Deficiencies were brought into this background, and the appropriate F<sub>1</sub> pupae were imaged at 18 h APF to determine whether there were any changes in pruning (Fig. 1F). Using this approach, we screened 135 deficiencies that cover ~80% of the third chromosome. On average, the deficiencies used removed ~40 genes. Our trans-heterozygous F<sub>1</sub>s fell into three distinct categories. One group showed wild-type pruning at 18 h APF (57 deficiencies of 135). Importantly, in this group there were F<sub>1</sub> genotypes in which a large number of genes, i.e., >140, were removed and pruning was found to be normal (Fig. 1G), suggesting that the loss of one copy of many different genes is not enough to generate pruning phenotypes. In the second category of deficiencies (34 deficiencies of 135), we observed clearance defects. In such trans-heterozygotes, severing appears to take place, and yet there is an increased frequency of hemisegments containing dendritic fragments (Fig. 1H). In the third category, we identified a number of deficiencies that resulted in severing defects (44 deficiencies of 135). In this group, dendrites were still found attached to the cell body at 18 h APF (Fig. 1I). Within the third group we identified the deficiency, Df(3R)ED5196, which removed *kat-60L1*, a gene that has been shown to be required for branch severing (Lee et al., 2009), suggesting that the screen is specific. We chose to focus on the third category, as severing is one of the first steps in pruning, and little is known about the molecular machinery that orchestrates it. Within this group we decided to further investigate Df(3R)ED6332 (Fig. 1J), as it removed only a small number of genes.

To identify the gene(s) responsible for the phenotype observed with Df(3R)ED6332, we expressed all of the available RNAi lines against the three genes covered by this deficiency and imaged the morphology of ddaC at 18 h APF. We found that two RNAi lines against the gene *headcase* (*hdc*), CG15532, were able

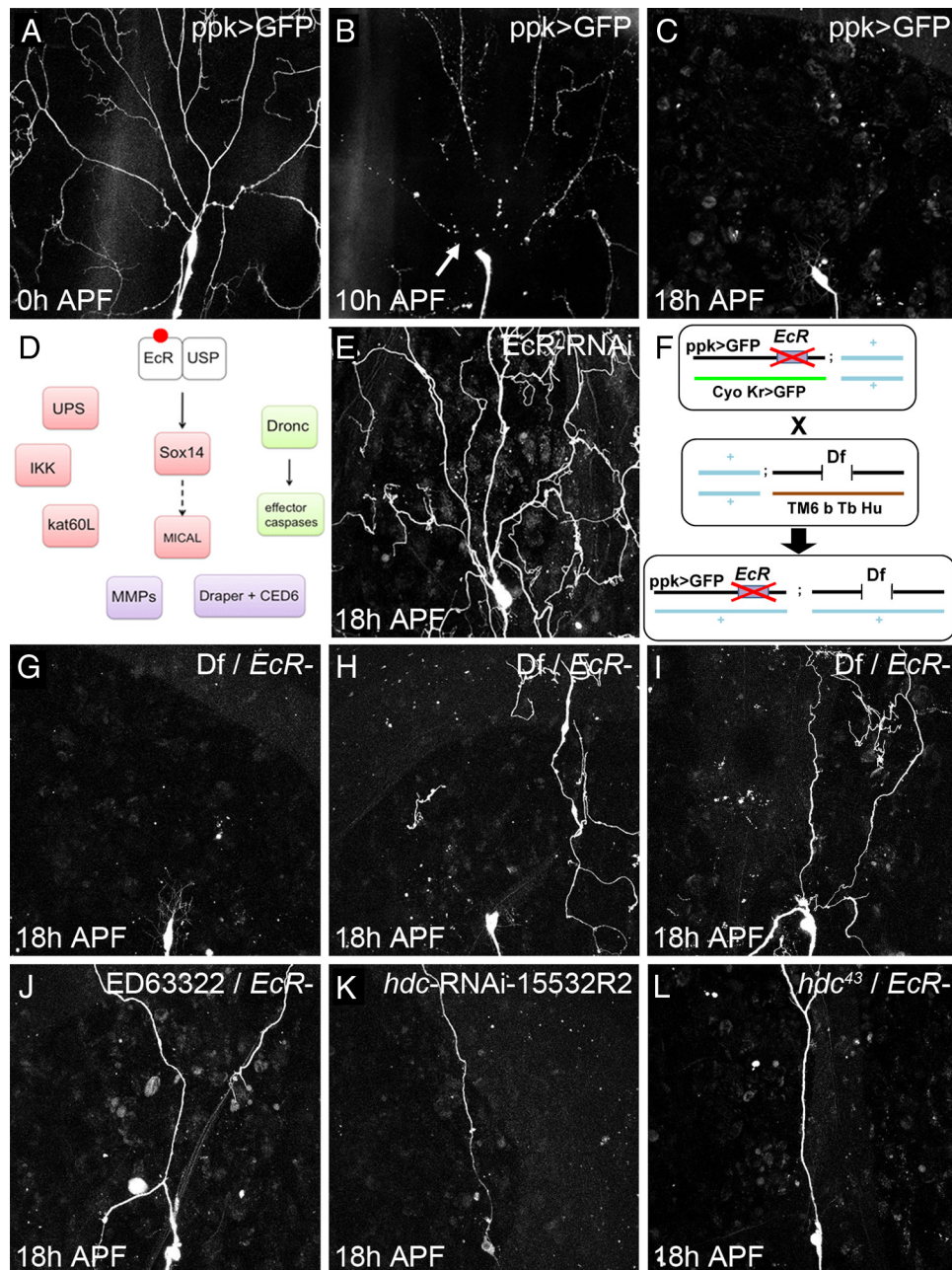


**Figure 1.** A screen to uncover new players of ddaC pruning. Live imaging of ddaC neurons labeled by ppk-GAL4 expressing UAS-CD8-GFP. **A–C**, A timeline of ddaC pruning. Z-projections of dorsal abdominal body wall at 0 (**A**), 10 (**B**), and 18 h APF (**C**), respectively. At 10 h APF, almost all the branches are severed close to the soma. By 18 h APF, the severed dendrites are cleared, only the soma and axon remain. **D**, Scheme showing the genes known to be involved in ddaC pruning; arrows represent direct interactions. **E**, The expression of EcR-RNAi<sup>CA104</sup> in ddaC robustly blocks the early stages of ddaC pruning. Dendritic branches are not severed at 18 h APF. **F**, Interaction screen: flies carrying ppk-GAL4, UAS-CD8-GFP, and a null mutation for EcR are crossed with balanced deficiencies. Pupal dominant markers on balancer chromosomes allow the selection of the appropriate genotypes. The F<sub>1</sub> pupae trans-heterozygous for EcR and a deficiency are imaged at 18 h APF and assessed for defects in pruning. **G–I**, ddaC neurons from pupae trans-heterozygous for EcR and three different deficiencies at 18 h APF. **G**, In category i of F<sub>1</sub> pupae, pruning is normal, meaning that there is no genetic interaction. **H** and **I** show F<sub>1</sub> pupae in which genetic interactions are evident. **H**, In category ii, clearance defects occur and pieces of dendrite are still in the field at 18 h APF; severing does not appear to be affected. **I**, In category iii, severing and clearance defects are evident with some dendrites still attached to the soma. **J–L**, Identification of the gene responsible for pruning defects within the deficiency Df(3R)ED6332. **J**, Trans-heterozygous neuron for Df(3R)ED6332 and EcR at 18 h APF. **K**, RNAi-15532R2, which targets *headcase* (*hdc*), one of the genes removed by Df(3R)ED6332, at 18 h APF. **L**, Genetic interaction between EcR and *hdc*<sup>43</sup>, a null allele of *hdc*, at 18 h APF.

to generate the severing defect (Fig. 1K). To confirm these results, we performed a genetic interaction test between EcR<sup>M554fs</sup> and two null alleles of headcase, *hdc*<sup>43</sup> (Fig. 1L) and *hdc*<sup>50</sup> (data not shown). Both alleles, when trans-heterozygous with EcR<sup>M554fs</sup>, recapitulate the severing defects (9%, *n* = 22 for *hdc*<sup>43</sup> and 37%, *n* = 8 for *hdc*<sup>50</sup>) observed with either the deficiency (16.7%, *n* = 6) or RNAi (80%, *n* = 10 for 15532R2). Taken together, these

data strongly suggest that the gene *headcase* is the causative factor within Df(3R)ED6332.

#### Spatial and temporal dynamics of *hdc*

To explore where and when *hdc* is expressed, we performed immunostaining with an antibody against HDC. *headcase* starts to be detectable in da sensory neurons only in late wandering third

instar larvae (wL3) (Fig. 2*B*). Its expression becomes stronger following puparium formation (0 h APF) (Fig. 2*C*) and is maintained until at least 5 h APF (Fig. 2*D*).

The staining reveals a cytoplasmic localization of HDC in da neurons, with an enrichment close to the nucleus. Although this perinuclear staining is intense, HDC is also present at lower levels in the dendrites and the axon. Between 0 and 5 h APF there is no obvious change in the localization of HDC within ddaC. Staining was found to be completely absent in homozygous null mutants (data not shown). We also observed staining in three of the neighboring sensory neurons (Fig. 2*C*, arrows). We tested HDC antibody on flies expressing an RNAi against *hdc* specifically in ddaC neurons. In these individuals, we saw a loss of HDC staining in these neurons, whereas HDC was still detectable in the neighboring da neurons (Fig. 2*E*). As a further control, we overexpressed HDC in ddaC neurons in flies which were homozygous mutants for *hdc*. Under these conditions, we observed a strong HDC staining only in ddaC neurons (Fig. 2*F*). In summary, *hdc* is expressed at a time and in a location that is compatible with a role in sensory neuron pruning.

### *hdc* is necessary for dendrite severing

The localization and onset of *hdc* expression in ddaC neurons and the targeted expression of RNAi tools designed to knock down *hdc* suggest that it may act in a cell-autonomous manner. To confirm this, we performed mosaic analysis with the MARCM system, generating ddaC neurons homozygous for a null allele of *hdc*.

Although we, along with others, have routinely used the MARCM system to investigate the cell-autonomous requirement of gene products during pruning, we felt the need to advance this approach. We combined a ppk-eGFP reporter construct with a nuclear localized RedStinger reporter under the control of the enhancer trap *elav*<sup>C155</sup>-GAL4. ppk-eGFP labels all class IV da neurons whether clonal or nonclonal, whereas the homozygous mutant clones are marked by *elav*<sup>C155</sup>-GAL4, which expresses strongly in the nervous system and also at low level in other tissues, including the epidermis. We have thus optimized the MARCM system to unequivocally identify our clones as ddaC neurons, visualize both the location and frequency of clones in neighboring tissues, and, importantly, compare our homozygous mutant ddaC clones with adjacent heterozygous control ddaC neurons in the same animal (Fig. 3*C*). To test this system, we used flies heterozygous for the null allele *esg*<sup>G66B</sup>, where ddaC pruning is wild type (data not shown). However, in pupae with MARCM clones, we either found heterozygous *esg* control (nonclonal) neurons that prune normally (Fig. 3*A*) or heterozygous neurons where pruning was strongly delayed (Fig. 3*B*). With our enhanced system we can now visualize and remove pupae with global developmental defects from our future analysis.

Using our modified MARCM technique, we performed clonal analysis with *hdc*<sup>43</sup>. We generated 16 pupae containing a single clonal (mutant) ddaC neuron and imaged the two adjacent nonclonal heterozygous ddaC neurons as controls (Fig. 3*C*). We observed severing defects in 50% of ddaC neurons homozygous mutant for *hdc* (Fig. 3*E*) where the neighboring control neurons were presenting no phenotype (Fig. 3*D,F*). Figure 3*E* is representative of how these severing phenotypes appear, with predominantly one or two dendrites remaining attached to the soma at 18 h APF. From these experiments, we conclude that *hdc* is required for the severing of dendrites in ddaC neurons and acts in a cell-autonomous manner.

### *hdc* is required but not sufficient for ddaC branch severing

As the expression of *hdc* coincides with the onset of dendritic pruning and is required cell autonomously for this process, we wanted to establish whether the precocious expression of *hdc* is sufficient to initiate branch severing. The expression of wild-type *headcase* from early larval life using ppk-GAL4 did not disrupt the development of the proximal dendrites of ddaC, and there was no evidence of degeneration or cell death (Fig. 4*A,C*). We then looked at the same animals following pupariation, when native *hdc* is expressed, to determine whether overexpression can cause precocious severing. We quantified the number of I° (branches located between the soma and the first branch point within the arborization) and II° branches (those from the first to the second branch point) still attached to the soma at 6 h APF. This proximal region was chosen because it is where severing normally takes place. At 0 h APF, the average number of I° and II° dendrites were similar between ppk-GAL4/w<sup>1118</sup> flies and ppk-GAL4>UAS-*hdc* flies with 10 ( $n = 21$ ) and 9 ( $n = 20$ ) dendrites, respectively. At 6 h APF, we found 6.2 and 5.2 dendrites in ppk-GAL4 ( $n = 38$ ) and ppk>UAS-*hdc* ( $n = 19$ ) flies, respectively. There was no statistically significant difference between the two groups ( $p = 0.3057$ ). We conclude that *hdc* overexpression during either larval life or soon after puparium formation is not sufficient to induce or accelerate dendrite severing.

### The short form of *hdc* is able to rescue *hdc* loss of function during pruning

A curious feature of *hdc* is the presence of a stop codon in the middle of the gene, allowing the generation of two distinct proteins from the same transcript. *headcase* generates a short form termed *hdcS* (70 kDa) and a full-length form (120 kDa) referred to as *hdcFL* (Steneberg et al., 1998). To determine which form was important during pruning, we performed rescue experiments that took advantage of the fact that homozygous mutant *hdc* animals can survive until late pupal stages, after pruning is completed. We used two transgenes, UAS-*hdc*Δ2, which allows the generation of a protein equivalent to *hdcS*, and UAS-*hdc*, which can produce both the full-length and the short form in flies (Steneberg et al., 1998). In homozygous *hdc*<sup>43</sup> animals we observed ~80% of ddaC neurons with severing defects at 18 h APF (Fig. 4*H,K*). The specific expression of either the UAS-*hdc* or UAS-*hdc*Δ2 transgene in ddaC neurons was able to rescue these defects at 18 h APF, with only 0–10% of the neurons showing a failure in severing (Fig. 4*I–K*). Although the short form generated by UAS-*hdc*Δ2 was sufficient to rescue *hdc* function in the severing of ddaC neurons, qualitative analyses showed that in around 80% of neurons the rescue was incomplete, with severed pieces of dendrites in the field for UAS-*hdc*Δ2 pupae against only 40% for UAS-HDC pupae (Fig. 4*H–J*). This data suggests that *hdc*Δ2 is sufficient to rescue ddaC pruning but is not as efficient as *hdcFL*.

### *headcase* is also required for pruning in other neuronal classes

During metamorphosis, larval neurons undergo remodeling or programmed cell death (Truman et al., 1990). Within the dorsal group of sensory neurons there are 6 da neurons, ddaA–F, which represent the four different classes of da neurons (Grueber et al., 2002). At the onset of metamorphosis, the class I da neurons, ddaD and ddaE, and class IV ddaC are remodeled, whereas the class II neuron ddaB and class III neurons ddaA and ddaF undergo apoptosis (Williams and Truman, 2005). To determine which of these neurons express *hdc*, we performed immunostain-

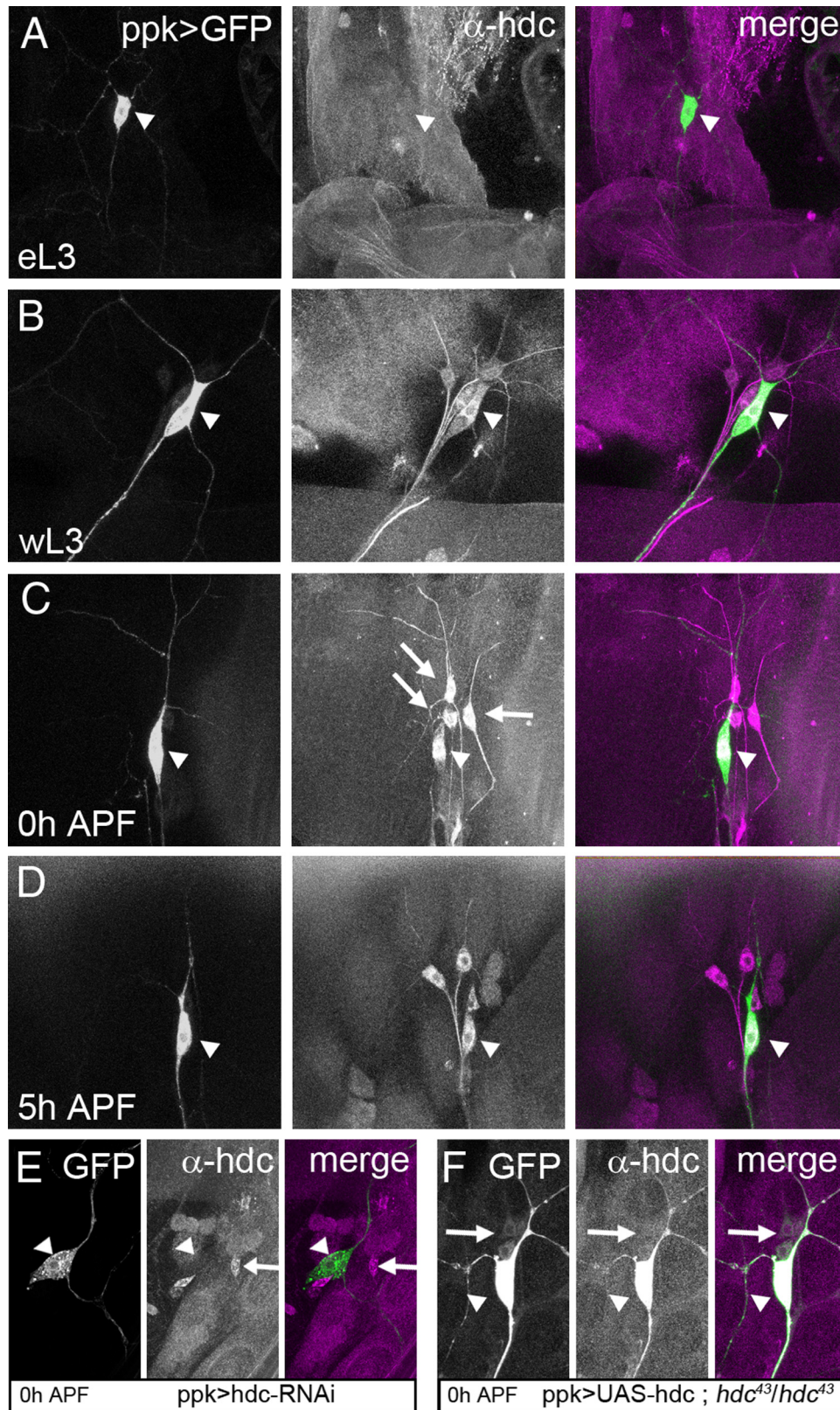


**Figure 2.** Spatial localization and temporal dynamics of *hdc* expression. **A–D**, Sensory neurons revealed by *ppk*-GAL4 driving UAS-CD8-GFP. These larval fillets are stained against HDC, and the GFP is observed without antibody. The arrowhead shows the position of *ddaC* neurons. **A**, *hdc* expression is not detectable in *ddaC* at early third instar larva (eL3). **B–D**, *hdc* expression starts during the wandering stage of L3 (wL3) (**B**), reaches a maximum at 0 h APF (**C**), and is still evident at 5 h APF (**D**). *hdc* is also expressed in some neighboring neurons (**C**, arrows). **E** and **F** are control experiments for HDC antibody. **E**, The specific expression of *hdc*-RNAi in *ddaC* neurons results in an absence of HDC staining (arrowhead), whereas this staining is still present in the neighboring *da* neurons (arrow). **F**, In *hdc*<sup>43</sup> homozygous mutant background, HDC staining is absent in *da* neurons (arrows) except in *ddaC* (arrowheads), where we are overexpressing HDC.

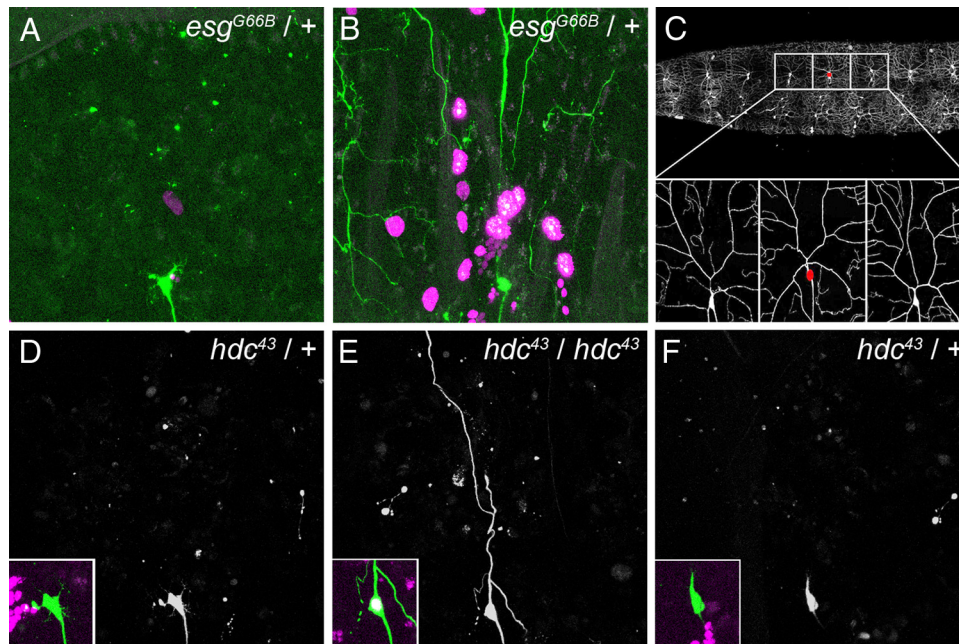


**Figure 3.** Cell-autonomous requirement of *hdc* in *ddaC* pruning. This figure shows live imaging of *ddaC* neurons labeled with *ppk-eGFP*; the MARCM clone is labeled with *UAS-RedStinger*, which provides a strong nuclear RFP signal, driven by *elav*<sup>C155</sup>-*GAL4*. **A** and **B** show two neurons from different 18 h APF pupae in which heat shocks were used to produce *esg*<sup>G66B</sup> MARCM clones. Neither of these neurons are MARCM clones, so they are heterozygous (*esg*<sup>G66B/+</sup>) and thus should not affect *ddaC* pruning. In **A**, the neuron undergoes wild-type pruning. In **B**, the neuron shows a strong pruning defect, not due to a cell autonomous effect but to a global developmental defect, as suggested by the high number of clonal epidermal cells expressing *RedStinger* (*esg*<sup>G66B</sup> homozygous; magenta nucleus). **C**, Modified MARCM strategy: selection of a MARCM clone *ddaC* neuron by its nuclear expression of *UAS-RedStinger* (red dot) and the two nonclonal neighboring neurons, which were used as controls. **D–F** show three adjacent *ddaC* neurons at 18 h APF belonging to the same pupa. **D** and **F** are not clonal, as they show no *RedStinger* expression (insets). The pruning of these neurons is wild type, and no pieces of dendrite are left in the field. The neuron in **E** is homozygous mutant for *hdc*, as revealed by *RedStinger* expression (inset). This neuron exhibits a severing defect, as a robust primary dendritic branch is still attached to the soma.

ing on all the multidendritic sensory neurons in the dorsal group labeled by the enhancer trap line C161-*GAL4*. We found that the class I, II, and III *da* neurons were *HDC* positive, alongside the dorsal bipolar dendrite neuron *dbd* (Fig. 5A–C).

To determine whether *hdc* is deployed in the remodeling of these neurons, we used the enhancer trap C161-*GAL4* to look at the effect of *hdc* loss of function in class I, II, and III *ddaA*, B, D, E, and F neurons. At 0 h APF we saw no obvious differences between these neurons in wild-type and *hdc* homozygous mutant flies, suggesting that their development does not depend on *hdc* (Fig. 5D and data not shown). By 24 h APF in wild-type flies, the larval dendrites of *ddaD*, *ddaE*, and *dbd* neurons were completely pruned back, whereas in *hdc*<sup>43</sup>/*hdc*<sup>43</sup> flies there were still a number of branches attached to the soma in 85% of the dorsal *da* groups ( $n = 20$ ) (Fig. 5E,F). At 24 h APF, *ddaA*, B, and F were absent in both wild-type and *hdc* mutant flies, revealing that the *hdc* function was not required for the programmed cell death of these neurons. Moreover, we found that the increased expression of *hdc* in *ddaA*, B, or F did not prevent their death (data not shown).

Mushroom body  $\gamma$ -MB neurons remodel their axons and dendrites during metamorphosis before elaborating their adult-specific projections (Watts et al., 2003). To determine whether *hdc* is required during  $\gamma$ -neuron pruning, we used the driver 201Y-*GAL4* to express *hdc*-RNAi. Alongside this, we generated homozygous *hdc*<sup>43</sup> MB neuroblast clones and visualized the morphology of mutant (*hdc*/*hdc*) at 24 h APF, when axonal and dendritic pruning is largely complete (Fig. 5G). We found no evidence for a disruption in the development of  $\gamma$ -MB neurons mutant for *hdc* (Fig. 5H,  $n = 8$ ), whereas expression of *EcR* RNAi with 201Y-*GAL4* leads to a robust block of pruning (Fig. 5I).

These data are consistent with a lack of *HDC* staining in  $\gamma$ -MB neurons (data not shown).

We conclude that *hdc* is involved in the pruning of different classes of sensory neurons but is not required in  $\gamma$ -MB neuron pruning, whereas *EcR* is required for pruning in both. We also find that removing *hdc* does not disrupt the programmed cell death of class II and III *da* neurons.

#### *hdc* is regulated by *EcR* but not by *Sox14*

Previous studies have shown that *headcase* can be regulated in imaginal tissues and the tracheal system by the transcription factors *escargot* (*esg*), *buttonhead* (*btd*), and *Sp1* (Steneberg et al., 1998; Estella et al., 2003). To determine whether any of these play a role in pruning, we generated *esg* mutant MARCM clones  $n = 10$  (Fig. 6A) and expressed RNAi against either *btd* or *Sp1* using the *ppk* driver (Fig. 6B, C). None of these regulators disrupted pruning in *ddaC*, suggesting that *hdc* is controlled differently in remodeling neurons.

As *hdc* expression closely follows the prepupal pulse of ecdysone, we asked whether *hdc* is regulated by ecdysone signaling. *EcR* was downregulated in *ddaC* by expressing *EcR*-RNAi<sup>CA104</sup> with *ppk*-*GAL4* (Fig. 1E). This cell-autonomous knockdown of *EcR* resulted in a lack of *hdc* expression at 0 h APF, when it is normally at its strongest (Fig. 6D). These data show that *hdc* is downstream of *EcR* and that it could be either a direct or indirect target. Recently, *Brahma* (*Brm*) and CREB binding protein (CBP) have been shown to be epigenetic factors that facilitate activation of downstream ecdysone response genes during pruning (Kirilly et al., 2011). The specific expression of a *Brm* or CBP dominant negative in *ddaC* results in a diminution of *hdc* expression at 0 h APF; this reduction is more pronounced with

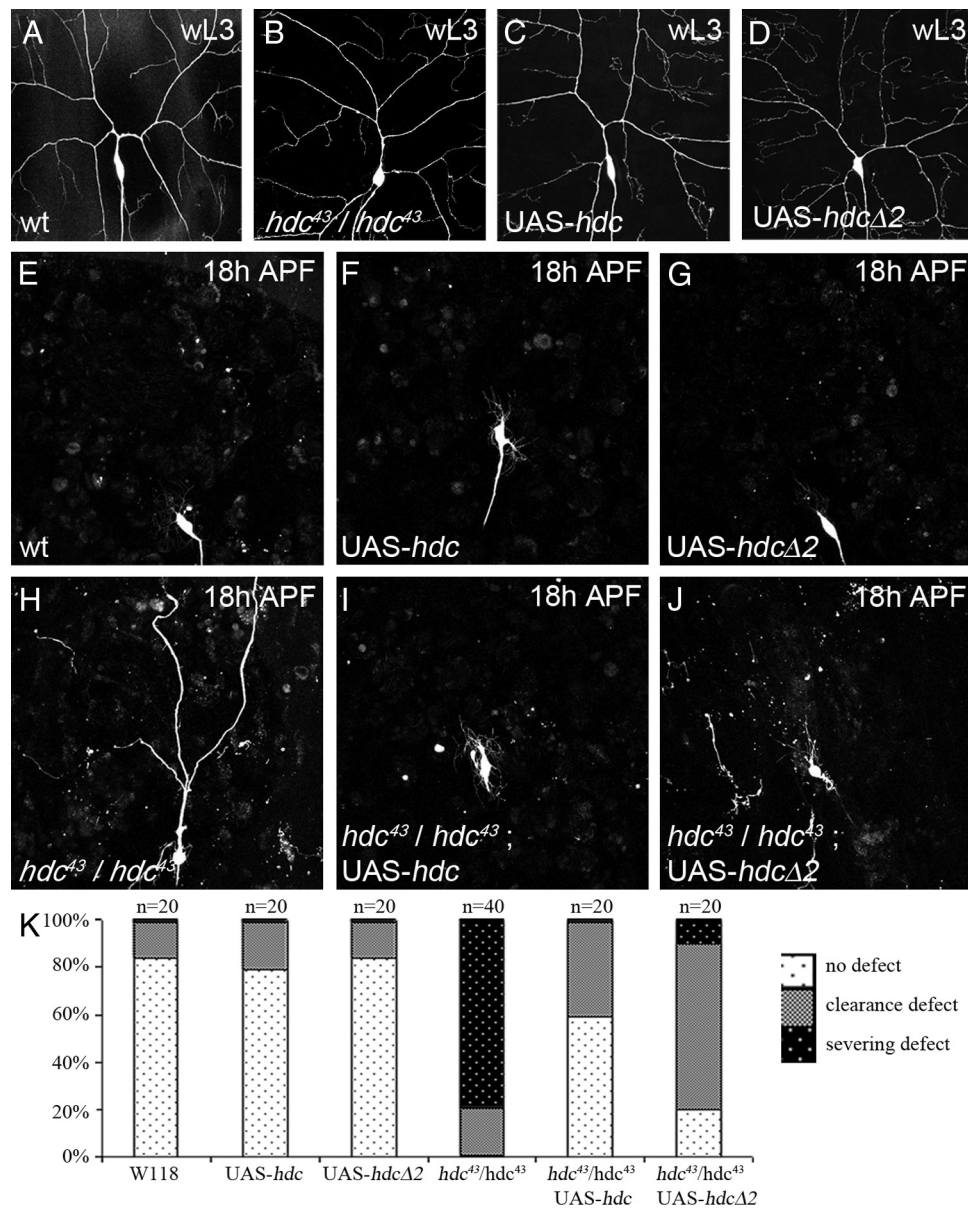


**Figure 4.** Both *hdc* forms work in pruning. ddaC neurons labeled with UAS-CD8-GFP driven by *ppk*-GAL4. This combination is also used to drive UAS-*hdc* or UAS-*hdc*Δ2. **A–D**, Panel showing that the number of I° and II° dendrites in ddaC neurons in wandering larvae (wL3), before pruning, does not appear to be modified in the different genotypes used for the gain-of-function experiments. **E–G**, Panel showing that at 18 h APF, ddaC neurons are pruned normally when overexpressing UAS-*hdc* or UAS-*hdc*Δ2. **H–J**, At 18 h APF, the strong severing defect found in *hdc<sup>43</sup>* homozygous background (**H**) is rescued by the expression of either UAS-*hdc* (**I**) or UAS-*hdc*Δ2 (**J**). There is more disruption of dendrite clearance in the UAS-*hdc*Δ2-rescued neurons (**J**). **K**, Quantification of both clearance and severing events confirming that both the short and the long forms of HDC can rescue *hdc<sup>43</sup>/hdc<sup>43</sup>* pruning in a significant manner ( $p < 0.0001$ ). Nevertheless, the short form (UAS-*hdc*Δ2) is less efficient than the expression of HDC full length.

CBP dominant negative (data not shown). Thus far, *Sox14* is the only direct target of EcR known to play a role in neuron pruning, and we wondered whether it could be controlling the expression of *hdc*. Previous work has demonstrated that RNAi against *Sox14* leads to a loss of *Sox14* staining and a strong severing phenotype in ddaC. However, this knockdown of *Sox14* does not seem to affect *hdc* expression in ddaC neurons (Fig. 6E), suggesting that *hdc* expression is independent of *Sox14*. Conversely, we found that *Sox14* expression was not affected in *hdc* mutant flies (Fig. 6F). Another possibility is that *hdc* could affect *Sox14* function. We used the expression of *Mical*, a target of *Sox14*, as a read-out for *Sox14* activity and found that *Mical* expression was also not modified in *hdc* mutant flies (data not shown).

These experiments suggest that *hdc* and *Sox14* belong to two parallel pathways downstream of EcR. To explore this idea further, we performed two additional functional assays. Firstly we expressed an RNAi against *Mical* in flies homozygous for *hdc<sup>43</sup>* and found that 100% of ddaC neurons had severing phenotypes and an average of 3.125 I° and II° dendrites attached to the soma (Fig. 7C). This is compared to 20% severing defects and 0.3 dendrites attached with *Mical*-RNAi alone (Fig. 7A) or 80% severing defects with 2.45 dendrites attached in homozygous *hdc<sup>43</sup>* alone (Fig. 7B). This reveals an additive phenotype for the double loss of function. Alongside this, the overexpression of *Mical* has previously been shown to partially rescue *Sox14* loss of function (Kirilly et al., 2009). We found that the overexpression of *hdc* in a *Sox14* loss-of-function background was unable to rescue the

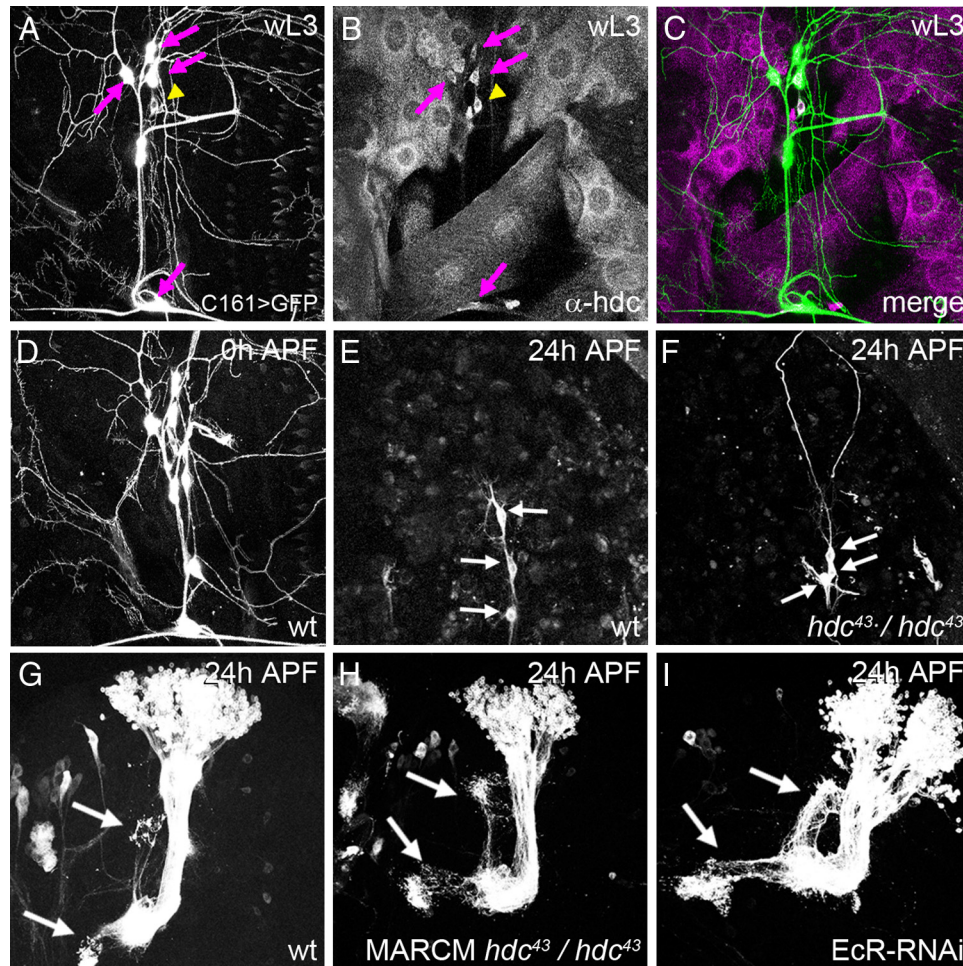


**Figure 5.** Role of *hdc* in other neurons that undergo remodeling. **A–C**, We used C161-GAL4 to express UAS-CD8::GFP in 5 other da neurons and stain the wL3 fillets with HDC antibody. *hdc* is expressed in the other class of da neurons, dbd neuron (purple arrows), and ddaC (yellow arrowhead). **D–F**, We used C161-GAL4 expressing UAS-CD8::GFP to visualize dorsal sensory neurons (**D**). In wild-type pupae at 24 h APF (**E**), only two da neurons and dbd neuron remain in the field (arrows), and they have undergone pruning. The three other da neurons labeled in C161-GAL4 have undergone apoptosis by this time. **F**, In *hdc<sup>43</sup>/hdc<sup>43</sup>* at 24 h APF, ddaA, B and F are absent, demonstrating that *hdc* is not required for the apoptosis of da neurons. The remaining neurons, ddaD, ddaE, and dbd, show consistent severing defects (arrows). **G–I**, Twenty-four hour APF  $\gamma$ -MB neurons labeled with 201Y-Gal4>UAS-mCD8-GFP. **G**,  $\gamma$ -MB neurons have almost completely pruned both their axons (arrows) and dendrites. **H**, In MARCM clones for *hdc<sup>43</sup>*, the pruning does not appear to be modified, and only a few axons remain (arrows). **I**, Pruning is suppressed by downregulating *EcR* with *EcR-RNAi*<sup>CA104</sup>, resulting in the persistence of axons at 24 h APF (arrows).

*Sox14* phenotype (Fig. 7D–G, J). Interestingly, we found that *hdc* overexpression limits the severing defects induced by *EcR-RNAi*<sup>CA104</sup> in ddaC at 18 h APF, even though they remain very strong (Fig. 7H–J). In a reverse experiment, we removed one copy of *EcR* in flies homozygous for *hdc<sup>43</sup>* and found that 94% of ddaC neurons had severing phenotypes with an average of 3.5 I° and II° dendrites remaining attached to the soma ( $n = 16$ ), compared to 80% with severing defects and 2.45 dendrites remaining in flies homozygous for *hdc<sup>43</sup>* ( $n = 40$ ). Taken together, these data strongly suggest that *hdc* and *Sox14* belong to different parallel pathways downstream of *EcR* in pruning neurons.

## Discussion

Large-scale pruning is deployed widely within the developing nervous system and yet little is known about the cellular and molecular mechanisms controlling it. This active removal of long neuronal processes is dynamic, with individual branches undergoing remodeling, severing, and clearance. Like programmed cell death, local branch-specific auto-destruction programs must be tightly regulated but also robust in their execution. We have exploited the metamorphic remodeling of the *Drosophila* sensory

system to develop an interaction screen that allowed us to identify *headcase*, a molecule that controls branch severing.

### A genetic interaction screen reveals a role for *hdc* in dendrite severing

Most of the genes involved in neuronal pruning have been identified using candidate-based approaches. With the exception of *Sox14*, these players are required for *EcR* expression (Lee et al., 1999; Schuldiner et al., 2008; Boulanger et al., 2011) or are relatively far downstream, i.e., direct regulators of the cytoskeleton (Lee et al., 2009). Our goal is to bridge this gap by identifying molecules that link *EcR* with these downstream targets. We established a genetic interaction screen that is both open ended and specific due to the detailed *in vivo* imaging of class IV dendritic arborizing sensory neurons. Interaction screens by their nature reveal targets that are in close genetic proximity. Here we used the null allele *EcR*<sup>M554fs</sup> as a sensitized background, as the ecdysone receptor sits at the apex of the pruning pathway. By focusing on disruptions to branch severing events, we have also biased the screen toward the discovery of molecules controlling the earliest steps of the pruning pathway. Using defined chromosomal defi-



ciencies, we removed large numbers of genes at a time and could then locate the gene of interest with relative ease. This strategy allowed us to identify headcase (*hdc*), CG15532, as the gene responsible for the severing phenotype. Previous work in *Drosophila* revealed that a loss of *hdc* disrupts the differentiation of imaginal primordia during pupal development and that its expression closely prefigures the re-entry of imaginal cells into the cell cycle (Weaver and White, 1995). Headcase is an evolutionarily conserved protein, and growing evidence suggests that the human homolog HECA plays a key role in carcinogenesis (Makino et al., 2001; Chien et al., 2006; Dowejko et al., 2009; Dowejko et al., 2012). It is a highly basic protein (pI, 9.6) and could therefore be involved in protein–protein or protein–RNA interactions. Currently, there are no obvious domains that give an indication of how HDC acts within the cell. This shows one of the benefits of such an open-ended screen, as we would clearly not have selected *hdc* using candidate-based approaches. We decided to explore its biological function and establish where it fits within the pruning pathway.

#### *hdc* acts cell autonomously during dendrite pruning

We have improved MARCM-based approaches for studying pruning in the remodeling of sensory neurons by using a GAL4-independent tool (ppk-eGFP) to visualize all class IV da sensory neurons in combination with a nuclear localized RedStinger protein to reveal MARCM clones (GAL80 minus). This approach has a number of advantages. Firstly, it allows the easy selection of clones and unequivocal identification of ddaC neurons. Secondly, it provides the opportunity to compare mutant ddaC clones with adjacent heterozygous ddaC “control neurons” within the same pupa. This is a robust internal control, which is particularly important as the long embryonic heat shocks used to generate mitotic clones within the sensory system also induce clones in many other tissues. As *elav*<sup>C155</sup>-*GAL4* also expresses *GAL4* in epidermal cells, it gives us insight into the global frequency of mitotic clones. Such “invisible” non-neural clones can disrupt the overall timing of puparium development, leading to non-cell autonomous effects on neuron pruning. With this modified version of the MARCM, we were able to account for these issues and confirm a cell-autonomous role for HDC in branch severing.

*hdc* overexpression did not result in precocious or accelerated severing, indicating that it is not a limiting factor. These data and the lack of known catalytic domain points toward HDC acting in concert with other factors in a complex.

#### *hdc* expression is regulated by *EcR* but not by *Sox14*

Our expression data show that *hdc* is expressed in da sensory neurons from the end of larval life. This immunostaining shows

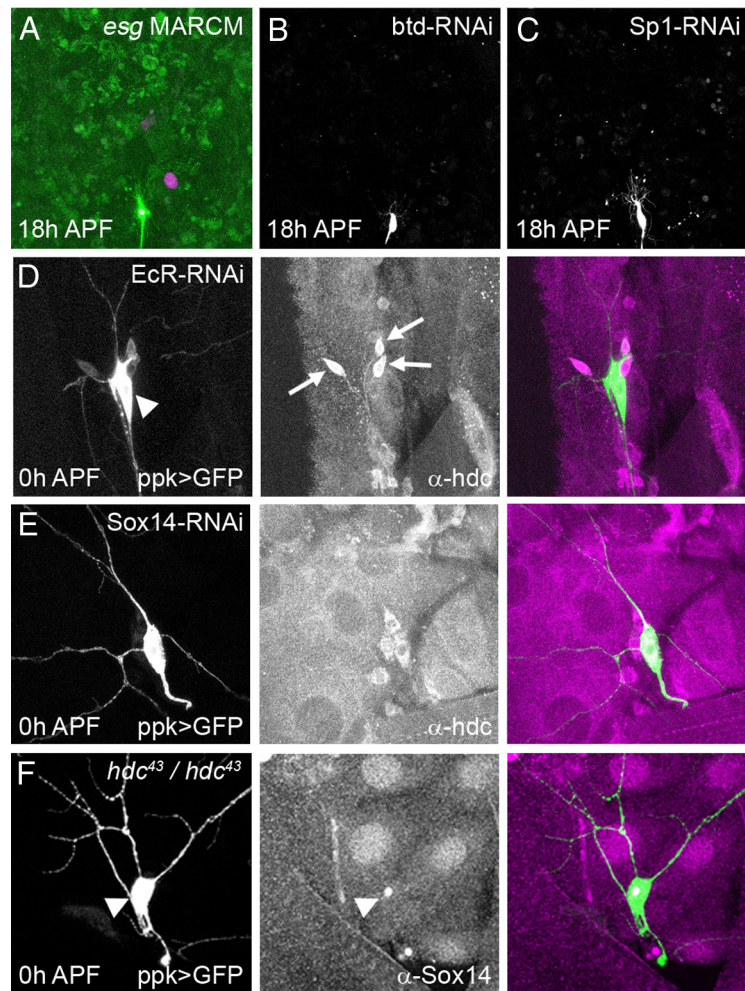


**Figure 6.** Regulation of *hdc* expression. **A**, MARCM clones for *esg*<sup>G66B</sup> show no defects in pruning at 18 h APF, (RedStinger expression in nucleus of homozygous mutant clone), **B**, **C**, ppk-GAL4>*btd*-RNAi (**B**) and ppk-GAL4>*Sp1*-RNAi (**C**) at 18 h APF; the pruning of ddaC neurons is not disrupted in either background. **D–F**, Fillets of 0 h APF pupa where ddaC neurons are labeled with UAS-CD8-GFP driven by ppk-GAL4, which is also used to drive *EcR*-RNAiCA104 or *Sox14*-RNAi when necessary. **D**, The expression of *EcR*-RNAiCA104 in ddaC neurons (arrowhead) suppresses *hdc* expression in a cell autonomous manner. HDC can still be seen in the neighboring da neurons (arrows). **E**, The expression of *Sox14*-RNAi in ddaC neurons does not affect *hdc* expression. **F**, In a *hdc*<sup>Δ3</sup>/*hdc*<sup>Δ3</sup> background, *Sox14* staining is still present in the nucleus of ddaC neurons (arrowhead).

that HDC is localized close to the nucleus, but not in it. It is also present at lower levels in proximal axons and dendrites. After branch severing begins, the majority of HDC remains perinuclear, suggesting that the specificity of HDC action is not likely to come from gross changes in its subcellular localization. The fact that *headcase* is not ubiquitously expressed but has a clear tissue-specific and temporal expression profile suggests that it is not a general factor but a notable component for gating the severing process. Normally, two forms of *headcase* are generated from a single transcript by a readthrough mechanism. Using transgenes, we find that both isoforms of HDC can rescue the pruning phenotype and that the long form is more effective. This mirrors the requirement for HDC function in the developing tracheal system (Steneberg et al., 1998; Steneberg and Samakovlis, 2001).

Previous studies have shown that *hdc* is regulated by buttonhead and *Sp1* in imaginal discs or by *escargot* in the trachea. We wondered if one of these transcription factors could also regulate *hdc* expression in ddaC neurons. The loss of function of these genes does not lead to any pruning defects, demonstrating that they are not required for *hdc* regulation within the peripheral

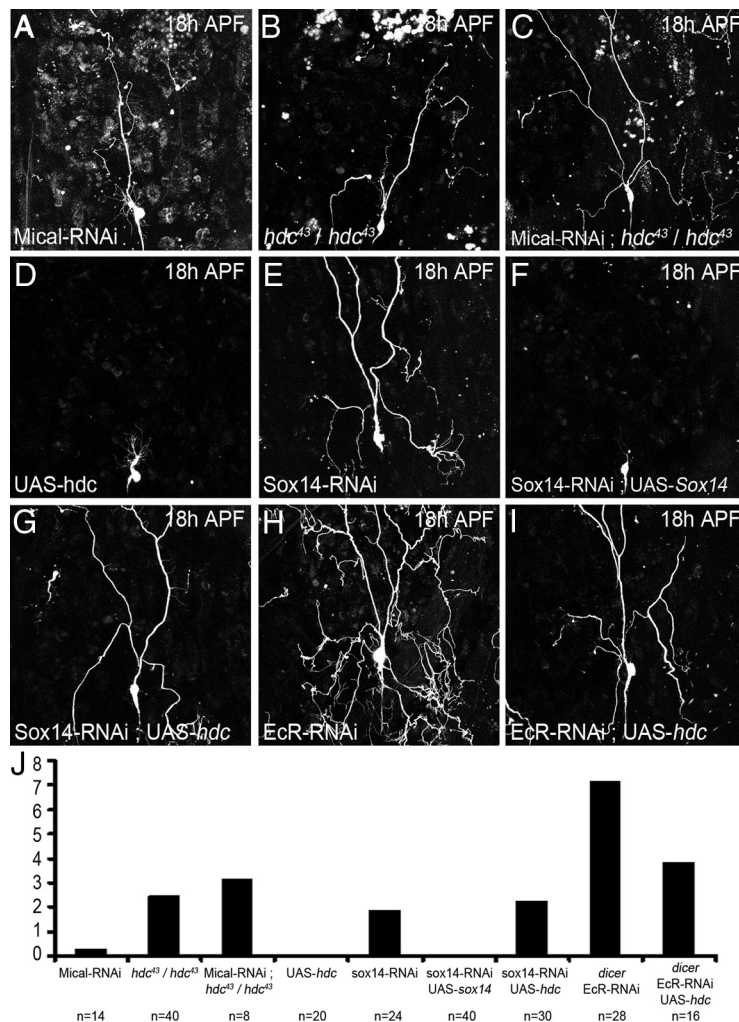


**Figure 7.** Epistasis experiments between *hdc*, *Sox14*, and *EcR*. ddaC neurons labeled with UAS-CD8-GFP driven by ppk-GAL4 at 18 h APF were also used to drive Mical-RNAi, UAS-*hdc*, *Sox14-RNAi*, UAS-*Sox14*, Mical-RNAi, and *EcR-RNAi*<sup>CA104</sup> alone or in combination. **A**, The expression of Mical-RNAi can lead to severing defect in 20% of ddaC neurons. **B**, Severing defect observed in 80% of flies homozygous for *hdc<sup>43</sup>*. **C**, The expression of Mical-RNAi in ddaC neurons of homozygous *hdc<sup>43</sup>* flies has an additive effect with 100% of the ddaC neurons presenting severing defect. **D**, *hdc* gain-of-function does not affect pruning of ddaC neurons. **E**, **F**, The strong severing defect observed with the expression of *Sox14-RNAi* (**E**) is completely rescued by the over expression of UAS-*Sox14* (**F**). **G**, The expression of UAS-*hdc* is not sufficient to rescue the severing defect generated by *Sox14-RNAi*. **H**, **I**, The almost complete suppression of pruning in ddaC neuron expressing *EcR-RNAi*<sup>CA104</sup> (**H**) is partially rescued by the overexpression of *hdc* (**I**). **J**, Quantification of 1° and 1° dendrites remaining attached to the soma. There is no significant difference between *Sox14-RNAi* and the combination of *Sox14-RNAi* and UAS-*hdc*. Although not total, the rescue of *EcR-RNAi*<sup>CA104</sup> phenotype by UAS-*hdc* is significant ( $p < 0.0001$ ).

nervous system. Thus, depending on the tissue, *hdc* seems to be regulated by different transcription factors. Importantly, the removal of *EcR* abolishes *hdc* expression in ddaC neurons, confirming that it is under the control of ecdysone signaling, downstream of *EcR* in the pruning pathway. It is unlikely that *hdc* is a direct target of *EcR* since it was never found in previous microarray analyses looking for *EcR* targets (Lee et al., 2003; Li and White, 2003; Beckstead et al., 2005). As *Sox14* is the only downstream transcription factor known to be involved in neuron pruning, we wanted to determine whether it could regulate *hdc* expression. Both immunostaining and rescue experiments lead us to the conclusion that there is no cross-regulation between *Sox14* and *hdc* in ddaC. Altogether, this data strongly supports the proposal that *hdc* and *Sox14* belong to two parallel pathways downstream of *EcR*. This observation of two and probably more independent pathways is consistent with the need for the precise

and active control of this auto-destructive machinery in different neuron types and different compartments within the cell.

#### *hdc* function is conserved in other classes of sensory neurons

To explore the role of *hdc* in other cell types, we looked at different neurons that remodel during metamorphosis. Our immunostaining revealed that *hdc* is expressed in all of the multidendritic (md) neurons we looked at, apart from *dmd1*. We found that loss of *hdc* function leads to a severing defect in class I and IV da sensory neurons and the dorsal bipolar dendrite neuron, *dbd*. Moreover, *hdc* loss or gain of function in class II and III da neurons does not change their fate, as they still undergo apoptosis (data not shown). We also found that *headcase* does not play a role in the  $\gamma$ -MB neuron pruning. This observation is interesting as we are looking at three distinct types of remodeling decisions within the fly nervous system: the loss of dendrites in ddaC pruning, the removal of both axons and dendrites in  $\gamma$ -MB, and cell death for class II and III da neurons. None of these appear to be a default state, because suppression of the pruning does not trigger apoptosis as seen in this study, nor does the blockage of cell death initiate branch severing (Williams and Truman, 2005). All three outcomes are triggered by the same ecdysone signal via *EcR* and one of its targets, *Sox14*. Here, we discovered a downstream target of the ecdysone signaling specific to dendrite pruning in a subset of remodeling neurons. This target is the founding member of a new pathway parallel to *Sox14*. We have exploited the metamorphic development of neurons and ecdysone signaling, which is of course specific to the phylum *Ecdyzoa*, but our expectation is that the batteries of downstream genes deployed during pruning are likely to be evolutionarily conserved and, thus, a useful entry point for investigating general principles of neurite pruning.

#### Conclusion

We have revealed for the first time that *hdc* is required in a cell-autonomous manner at the severing step during md neuron pruning. Importantly, our data also reveals that *hdc* acts independently of *Sox14*, despite both being under the control of *EcR*. These observations highlight that pruning is an association of multiple parallel pathways downstream of *EcR*.

Furthermore, we show through the identification of *hdc* that we have developed a genetic interaction screen that is an efficient and elegant way to populate the pruning pathway. This is a fundamental step toward understanding the complex regulation of this active and tightly regulated auto-destruction process.

## References

- Beckstead RB, Lam G, Thummel CS (2005) The genomic response to 20-hydroxyecdysone at the onset of *Drosophila* metamorphosis. *Genome Biol* 6:R99. [CrossRef Medline](#)
- Boulanger A, Clouet-Redt C, Farge M, Flandre A, Guignard T, Fernando C, Juge F, Dura JM (2011) *ftz-fl* and *Hr39* opposing roles on EcR expression during *Drosophila* mushroom body neuron remodeling. *Nat Neurosci* 14:37–44. [CrossRef Medline](#)
- Chien CC, Chang CC, Yang SH, Chen SH, Huang CJ (2006) A homologue of the *Drosophila* headcase protein is a novel tumor marker for early-stage colorectal cancer. *Oncol Rep* 15:919–926. [Medline](#)
- Dietzl G, Chen D, Schnorrrer F, Su KC, Barinova Y, Fellner M, Gasser B, Kinsey K, Oettel S, Scheiblaue S, Couto A, Marra V, Keleman K, Dickson BJ (2007) *Nature* 448:151–156. [CrossRef Medline](#)
- Dowjko A, Bauer RJ, Muller-Richter UD, Reichert TE (2009) The human homolog of the *Drosophila* headcase protein slows down cell division of head and neck cancer cells. *Carcinogenesis* 30:1678–1685. [CrossRef Medline](#)
- Dowjko A, Bauer R, Bauer K, Muller-Richter UD, Reichert TE (2012) The human HECA interacts with cyclins and CDKs to antagonize Wnt-mediated proliferation and chemoresistance of head and neck cancer cells. *Exp Cell Res* 318:489–499. [CrossRef Medline](#)
- Elfring LK, Daniel C, Papoulas O, Deuring R, Sarte M, Moseley S, Beek SJ, Waldrip WR, Daubresse G, DePace A, Kennison JA, Tamkun JW (1998) Genetic analysis of *brahma*: the *Drosophila* homolog of the yeast chromatin remodeling factor SWI2/SNF2. *Genetics* 148:251–265. [Medline](#)
- Estella C, Rieckhof G, Calleja M, Morata G (2003) The role of *buttonhead* and *Sp1* in the development of the ventral imaginal discs of *Drosophila*. *Development* 130:5929–5941. [CrossRef Medline](#)
- Grueber WB, Jan LY, Jan YN (2002) Tiling of the *Drosophila* epidermis by multidendritic sensory neurons. *Development* 129:2867–2878. [Medline](#)
- Grueber WB, Jan LY, Jan YN (2003) Different levels of the homeodomain protein *cut* regulate distinct dendrite branching patterns of *Drosophila* multidendritic neurons. *Cell* 112:805–818. [CrossRef Medline](#)
- Hayashi S (1996) A *Cdc2* dependent checkpoint maintains diploidy in *Drosophila*. *Development* 122:1051–1058. [Medline](#)
- Kirilly D, Gu Y, Huang Y, Wu Z, Bashirullah A, Low BC, Kolodkin AL, Wang H, Yu F (2009) A genetic pathway composed of *Sox14* and *Mical* governs severing of dendrites during pruning. *Nat Neurosci* 12:1497–1505. [CrossRef Medline](#)
- Kirilly D, Wong JJ, Lim EK, Wang Y, Zhang H, Wang C, Liao Q, Wang H, Liou YC, Yu F (2011) Intrinsic epigenetic factors cooperate with the steroid hormone ecdysone to govern dendrite pruning in *Drosophila*. *Neuron* 72:86–100. [CrossRef Medline](#)
- Kumar JP, Jamal T, Doetsch A, Turner FR, Duffy JB (2004) CREB binding protein functions during successive stages of eye development in *Drosophila*. *Genetics* 168:877–893. [CrossRef Medline](#)
- Kuo CT, Jan LY, Jan YN (2005) Dendrite-specific remodeling of *Drosophila* sensory neurons requires matrix metalloproteases, ubiquitin-proteasome, and ecdysone signaling. *Proc Natl Acad Sci U S A* 102:15230–15235. [CrossRef Medline](#)
- Kuo CT, Zhu S, Younger S, Jan LY, Jan YN (2006) Identification of E2/E3 ubiquitinating enzymes and caspase activity regulating *Drosophila* sensory neuron dendrite pruning. *Neuron* 51:283–290. [CrossRef Medline](#)
- Lee CY, Clough EA, Yellon P, Teslovich TM, Stephan DA, Baehrecke EH (2003) Genome-wide analyses of steroid- and radiation-triggered programmed cell death in *Drosophila*. *Curr Biol* 13:350–357. [CrossRef Medline](#)
- Lee HH, Jan LY, Jan YN (2009) *Drosophila* IKK-related kinase *Ik2* and *Katanin p60-like 1* regulate dendrite pruning of sensory neuron during metamorphosis. *Proc Natl Acad Sci U S A* 106:6363–6368. [CrossRef Medline](#)
- Lee T, Luo L (1999) Mosaic analysis with a repressible cell marker for studies of gene function in neuronal morphogenesis. *Neuron* 22:451–461. [CrossRef Medline](#)
- Lee T, Lee A, Luo L (1999) Development of the *Drosophila* mushroom bodies: sequential generation of three distinct types of neurons from a neuroblast. *Development* 126:4065–4076. [Medline](#)
- Lee T, Marticke S, Sung C, Robinow S, Luo L (2000) Cell-autonomous requirement of the USP/EcR-B ecdysone receptor for mushroom body neuronal remodeling in *Drosophila*. *Neuron* 28:807–818. [CrossRef Medline](#)
- Li TR, White KP (2003) Tissue-specific gene expression and ecdysone-regulated genomic networks in *Drosophila*. *Dev Cell* 5:59–72. [CrossRef Medline](#)
- Lin DM, Fetter RD, Kopczynski C, Grenningloh G, Goodman CS (1994) Genetic analysis of *Fasciclin II* in *Drosophila*: defasciculation, refasciculation, and altered fasciculation. *Neuron* 13:1055–1069. [CrossRef Medline](#)
- Luo L, O'Leary DD (2005) Axon retraction and degeneration in development and disease. *Annu Rev Neurosci* 28:127–156. [CrossRef Medline](#)
- Makino N, Yamato T, Inoue H, Furukawa T, Abe T, Yokoyama T, Yatsuoka T, Fukushige S, Orikasa S, Takahashi T, Horii A (2001) Isolation and characterization of the human gene homologous to the *Drosophila* headcase (*hdc*) gene in chromosome bands 6q23–q24, a region of common deletion in human pancreatic cancer. *DNA Seq* 11:547–553. [Medline](#)
- Mason C (2009) The development of developmental neuroscience. *J Neurosci* 29:12735–12747. [CrossRef Medline](#)
- Nakamura H, O'Leary DD (1989) Inaccuracies in initial growth and arborization of chick retinotectal axons followed by course corrections and axon remodeling to develop topographic order. *J Neurosci* 9:3776–3795. [Medline](#)
- Portera-Cailliau C, Weimer RM, De Paola V, Caroni P, Svoboda K (2005) Diverse modes of axon elaboration in the developing neocortex. *PLoS Biol* 3:e272. [CrossRef Medline](#)
- Schubiger M, Wade AA, Carney GE, Truman JW, Bender M (1998) *Drosophila* EcR-B ecdysone receptor isoforms are required for larval molting and for neuron remodeling during metamorphosis. *Development* 125:2053–2062. [Medline](#)
- Schubiger M, Carré C, Antoniewski C, Truman JW (2005) Ligand-dependent de-repression via EcR/USP acts as a gate to coordinate the differentiation of sensory neurons in the *Drosophila* wing. *Development* 132:5239–5248. [CrossRef Medline](#)
- Schuldiner O, Berdnik D, Levy JM, Wu JS, Luginbuhl D, Gontang AC, Luo L (2008) piggyBac-based mosaic screen identifies a postmitotic function for cohesin in regulating developmental axon pruning. *Dev Cell* 14:227–238. [CrossRef Medline](#)
- Shepherd D, Smith SA (1996) Central projections of persistent larval sensory neurons prefigure adult sensory pathways in the CNS of *Drosophila*. *Development* 122:2375–2384. [Medline](#)
- Stanfield BB, O'Leary DD, Fricks C (1982) Selective collateral elimination in early postnatal development restricts cortical distribution of rat pyramidal tract neurones. *Nature* 298:371–373. [CrossRef Medline](#)
- Steneberg P, Samakovlis C (2001) A novel stop codon readthrough mechanism produces functional Headcase protein in *Drosophila* trachea. *EMBO Rep* 2:593–597. [CrossRef Medline](#)
- Steneberg P, Englund C, Kronhamn J, Weaver TA, Samakovlis C (1998) Translational readthrough in the *hdc* mRNA generates a novel branching inhibitor in the *Drosophila* trachea. *Genes Dev* 12:956–967. [CrossRef Medline](#)
- Truman JW (1990) Metamorphosis of the central nervous system of *Drosophila*. *J Neurobiol* 21:1072–1084. [CrossRef Medline](#)
- Truman JW, Reiss SE (1976) Dendritic reorganization of an identified motoneuron during metamorphosis of the tobacco hornworm moth. *Science* 192:477–479. [CrossRef Medline](#)
- Truman JW, Fahrbach SE, Kimura K (1990) Hormones and programmed cell death: insights from invertebrate studies. *Prog Brain Res* 86:25–35. [CrossRef Medline](#)
- Truman JW, Schuppe H, Shepherd D, Williams DW (2004) Developmental architecture of adult-specific lineages in the ventral CNS of *Drosophila*. *Development* 131:5167–5184. [CrossRef Medline](#)
- Watts RJ, Hoopfer ED, Luo L (2003) Axon pruning during *Drosophila* metamorphosis: evidence for local degeneration and requirement of the ubiquitin-proteasome system. *Neuron* 38:871–885. [CrossRef Medline](#)
- Weaver TA, White RA (1995) *headcase*, an imaginal specific gene required for adult morphogenesis in *Drosophila melanogaster*. *Development* 121:4149–4160. [Medline](#)
- Williams DW, Shepherd D (1999) Persistent larval sensory neurons in adult *Drosophila melanogaster*. *J Neurobiol* 39:275–286. [CrossRef Medline](#)
- Williams DW, Truman JW (2004) Mechanisms of dendritic elaboration of sensory neurons in *Drosophila*: insights from in vivo time lapse. *J Neurosci* 24:1541–1550. [CrossRef Medline](#)
- Williams DW, Truman JW (2005) Cellular mechanisms of dendrite pruning in *Drosophila*: insights from in vivo time-lapse of remodeling dendritic arborizing sensory neurons. *Development* 132:3631–3642. [CrossRef](#)

Williams DW, Kondo S, Krzyzanowska A, Hiromi Y, Truman JW (2006) Local caspase activity directs engulfment of dendrites during pruning. *Nat Neurosci* 9:1234–1236. CrossRef Medline

Yang MY, Armstrong JD, Vilinsky I, Strausfeld NJ, Kaiser K (1995) Subdivision of the *Drosophila* mushroom bodies by enhancer-trap expression patterns. *Neuron* 15:45–54. CrossRef Medline